Control of Inherent Vibration of Flexible Robotic Systems and Associated Dynamics

Debanik Roy

Abstract The domain of Flexible Robotic Systems (FRS) is one of the unique ensembles of robotics research that deals with various modes of vibrations, inherent in the system. The vibration, so referred, is completely built-in type and thus it is designed invariant. By nature, the vibration in FRS is self-propagating and does not follow analytical modeling and rule-base in all applications. The asynchronous data fusion, emanating out of FRS is a challenging research paradigm till date, primarily due to the inherent characteristics in quantifying the output response of the system. Real-time assessment of vibration signature in FRS is a prerequisite for establishing a reliable control system for any real-life application. The paper focuses on a new approach of modeling this inherent vibration of the flexible robotic system and brings out its effect on the associated dynamics of the FRS. Besides, the paper dwells on modeling and theoretical analysis for a novel rheological rule-base, centering on the zone-based relative dependency of the finite numbered sensor units in combating the inherent vibration in the flexible robot. Besides, a new proposition is developed for assessing the decision threshold band, signaling the activation of the FRS-gripper, using a stochastic model.

Keywords Flexible robot · Vibration · Rheology · Data fusion · Sensor · Hypothesis · Algorithm

1 Introduction

Characterization and dynamic analysis of Flexible Robotic Systems (FRS) is a challenging arena of today's robotics research as the system is gaining foothold for a variety of applications in social and medical diagnosis. Although FRS is having an advantage of very low tare weight which is quite befitting for a large number of applications, yet the major bottleneck is its inherent vibration. This inherent vibration is a

D. Roy (✉)
Division of Remote Handling and Robotics, Bhabha Atomic Research Centre, Mumbai, India
e-mail: deroy@barc.gov.in

Department of Atomic Energy, Homi Bhabha National Institute, Mumbai, India

S. Chakraverty and P. Biswas (eds.), *Recent Trends in Wave Mechanics and Vibrations*, Lecture Notes in Mechanical Engineering,
https://doi.org/10.1007/978-981-15-0287-3_16

totally built-in type, structure independent and gets manifested in two ways, namely, modal frequency and eigenvalue. Several designs of FRS have been attempted by the researchers in past decade in order to alleviate this vibration but most of those trials have been unsuccessful. The problem gets even complicated when we attempt for multi-link design of the FRS, wherein various kinds of coupled effect and nonlinearity crave in. It has been also observed that vibration in FRS is not time-dependent and the duration and periodicity of it cannot be correlated with the task space of the robotic system. Moreover, by nature, this vibration is self-propagating and it gets induced to the successive member of the FRS till the end-link as well as the end-effector/gripper. At times, vibration becomes self-generating and random too. Due to all these characteristics, it is very difficult to obtain a generic analytical model for the vibration in FRS. And, since modeling cannot be attempted in a generic manner, usual rule-bases for adopting control algorithm for the end-applications are also unviable.

The other issue, pertaining to analyzing this self-induced built-in vibration in FRS, is the modality of fusing the real-time data on vibration (amplitude and frequency). Since we need to evolve with a robust system for reducing this vibration and effect thereon, there is a need to design a system for asynchronous data fusion. Unlike the traditional approaches of sensory data fusion, FRS-based data fusion has another dimension for the analysis, viz., time-period, thereby signifying real-time operation of the FRS. In totality, this asynchronous data fusion ensemble has evolved as a challenging open research paradigm in recent past. Proper quantification of the output response, i.e., vibration signature is one of the challenges in executing the FRS. The problem gets even critical when we need to deal with multiple links of the FRS and/or limited number of elemental sensor units, in contrast to traditional theories dealing with robust structural dynamics of Industrial Robotic Systems (IRS).

In all practical applications, the vibration signature in FRS gets assessed through multiple force sensors, spread over the links, and joints of the FRS in real time. The sensory data, so generated, is fed to a fusion model and the outcome becomes instrumental in establishing a reliable control system for the FRS. It is imperative that relatively better vibration signature can be obtained by agglomerating identical sensor units.

In this paper, we will focus on a new approach of modeling this inherent vibration of the FRS and discuss its effect on the associated dynamics of the flexible robotic system. In fact, vibration models used hitherto in FRS have been found to be somewhat inappropriate for real-time monitoring and control of the payload, i.e., the object to be gripped at the end-of-arm tooling. Besides, the dynamics effect due to link-wise (zonal) distribution of the sensors in the FRS was largely unattended.

In answering those lacunas, the present paper dwells on the modeling, algorithm, and theoretical analysis of a novel rheological rule-base, centering on the zone-based relative dependency of the finite numbered sensor units in combating the inherent vibration in the flexible robot. Besides, a new proposition is developed for assessing the decision threshold band, signaling the activation of the FRS-gripper, using a stochastic model.

Control issues of FRS have gained research attention over the last few decades, which deal with novel techniques of control of system dynamics in real time [1]. While perturbation method was tried for fine-tuning FRS-controller [2], direct real-time feedback from strain gauges was experimented too [3]. It is true that a robust dynamic model becomes very effective in understanding the behavior of FRS in real time and the same becomes crucial for a multi-link FRS [4, 5]. Feliu et al. attempted the control issue of a three degrees-of-freedom FRS using the methodology of inverse dynamics in contrast to strain gauge-based control [6, 7]. The fuzzy learning-based approach for control of FRS was also reported by Moudgal et al. [8]. Specific metrics related to reduction of system vibration of a robotic gadget were attributed by Singer and Seering [9]. Various techniques for vibration attenuation and control in FRS have been reported hitherto, such as sliding mode theory [10], adaptive resonant control [11], online frequency and damping estimation [12], and integral resonant control [13]. Dynamic model and simulation of FRS based on spring and rigid bodies was established too [14]. However, modeling of the multi-link FRS using compliant subassemblies, such as spring-dashpot-damper, remains an open research domain till date.

It is to be noted that in experimental mode of modeling and control of in situ vibration of FRS needs a strong encapsulation of data structure, data assimilation and finally, statistical analysis. Attainment of optimality in data fusion and decision fusion are two important facets in this context [15, 16]. Likewise, theories of Bayesian detection [17] and Adaptive decision [18] have been reported. Stochastic modeling and novel hypothesis testing-based decision theory have been delineated in [19]. Various application metrics of the developed hypothesis testing-based decision thresholding have been reported, viz., dissimilar sensor-cells in robotic gripper sensor [20], robotic slip sensory grid [21], and field robotic sensory system [22, 23]. Based on the earlier attainments, we will propose here a new fusion rule-base for the real-time analysis of vibration data of FRS.

The paper has been organized into seven sections. An overview of the firmware of the multi-degrees-of-freedom FRS is presented in the next section. Details on the possible sources of vibration in the flexible robotic system and characteristics of such vibration have been discussed in Sect. 3. Issues related to modeling on the real-time damping and dynamics are attributed in Sect. 4. Paradigms on data analysis with respect to dynamic control and stability of the FRS are discussed in Sect. 5. Simulation results for evaluating the vibration characteristics of the flexible robot, along with its hardware (prototype), are reported in Sect. 6 and finally, Sect. 7 concludes the paper.

2 Firmware of Multiple Degrees-of-Freedom Flexible Robotic Systems

Although flexible robots have become favorable choice in several new applications because of slender design, lightweight, small size envelope, and increased reachability in the workspace, yet the major bottleneck of the system lies with the effective control of inherent vibration. A widely accepted engineering way of evaluating this vibration is to detect and measure the deflection of the FRS-member(s) in real time. The formulation, modeling, and instrumentation for such deflection measurement are pre-characterized and can be adopted with the help of miniature strain gauges and flexi-force sensors.

One important design aspect of small-sized FRS is to augment drive mechanisms at the base of the robot, in order to reduce the tare weight of the link subassemblies. Although it is possible to integrate miniature servomotor(s) at the respective joint-link interface of the FRS, our experience says that such FRS will prone to have unwarranted drooping from time to time during its actuation, which will degenerate in additional trembling of the FRS-ensemble. Hence, even though in situ motor-driven (direct drive) FRS is compact in hardware, it is not the ideal design choice. In order to alleviate this problem, the optimal design approach is to use flexible shaft for the joint actuation. Flexible shafts transmit rotary motion over, under, and around "obstacles". They have higher efficiencies and are more economical than gears, universal joints, belts, and pulleys. By this modus operandi, all drive motors will be placed at the base of the FRS and respective joint will be actuated through flexible shaft, connected between the motor-output-shaft and the joint-shaft. Figure 1 schematically illustrates the layout of a serial-chain two-link FRS, fitted with flexible shafts. The tapered cross section of the links has been conceived to have less weight and better slenderness ratio. The FRS is having two links and two revolute type joints with no joint at the wrist. While the motor tuple {M1 and M2} is located at the base of the FRS, the motor, M3 is responsible for the operation of the micro-gripper.

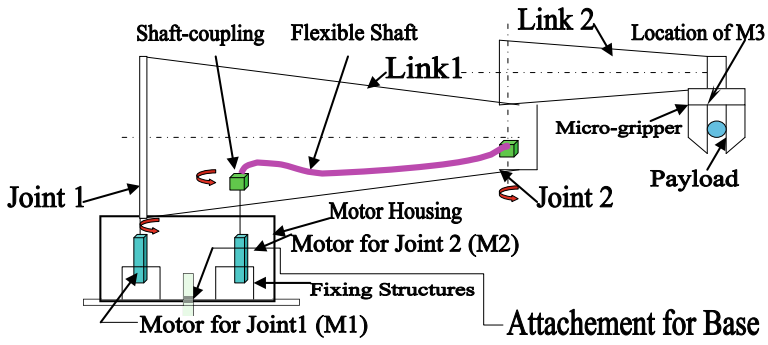

Fig. 1 Layout of the serial-chain flexible manipulator with flexible shaft mechanism

The drive for joint 1 is direct, i.e. coupled straight away with M1. The drive for joint 2 is through the flexible shaft. The driver end (left hand side) of the flexible shaft is the shaft of M2 and the transmission is carried over to the driven end of the shaft (right-hand side) and thereafter to the joint. The system is to be mounted on a customized mechanism beneath the base, namely, the part, labeled as "attachment for base" in Fig. 1. This is a sort of prismatic mechanism, positioned on a tripod, having linear movements along vertical Z-axis. Figure 2 illustrates a schematic view of the mechanism.

A standard flexible shaft, as available commercially, is shown in Fig. 3a. The major design estimation is its Length, i.e., "L" as per the sketch. The overall length must be determined by closely approximating all bends and offsets. Also, the length of the flexible shaft should be measured along the centerline of the shaft. In other words, in case of flexible robot, "L" should be selected considering enough clearance apart from the normal distance of separation between Joint 1 and Joint 2. The bend radius (R) is an important dimension of a flexible shaft mechanism, besides other two dimensions; namely, "X" and "Y" (refer Fig. 3b for details). While "X" is to be selected based on the total span of transfer of drive from joint to link of the FRS; "Y" will be instrumental in combating torsion of the flexible shaft and link thereof.

The firmware of serial-chain FRS with three links and two flexible shafts is very crucial from the angle of system dynamics and control of vibration. Figure 4 presents

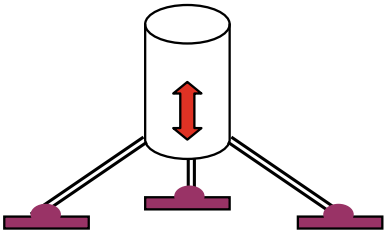

Fig. 2 Schematics of the prismatic mechanism at FRS-base

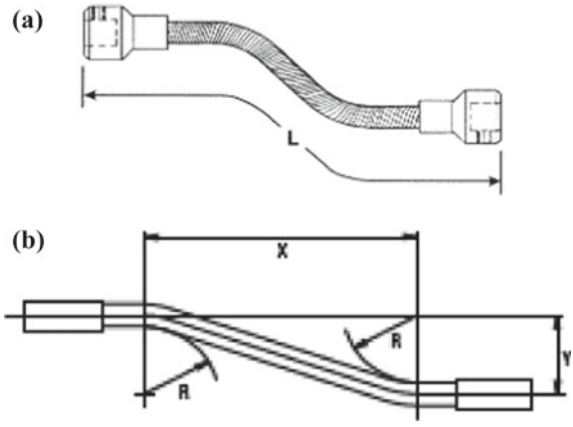

Fig. 3 **a**. Representative view of a flexible shaft. **b**. Representative critical design of a flexible shaft

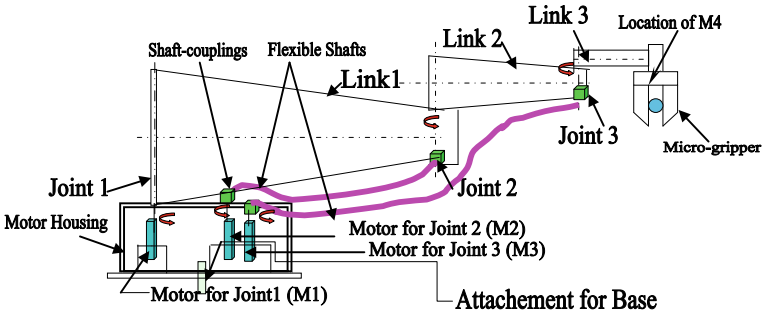

Fig. 4 Schematic of the three-link serial-chain planar type flexible robot with two flexible shafts

the overall schematic of the design, wherein motor for the third joint (M3) will also be at the base, along with M1 and M2. The motor responsible for the actuation of the gripper is indexed as M4 here. The final prototype is to be made in modular fashion ideally, so that links can be detached easily as and when required in order to smoothen the dynamics in real time.

With reference to Figs. 1 and 4, it is to be noted that actual dimensions of the tapered links are in mm range and much smaller than the visual impressions of the sizes. The revolute joints need to be constructed as simple bearing-supported pin joints, with an extended flange at the bottom. Figure 5 presents the detailed schematic of the revolute joint to be fabricated.

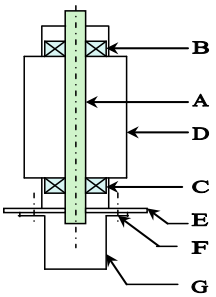

Legends: **A**: Pin; **B**: Micro-Bearing (Upper Rung); **C**: Micro-Bearing (Lower Rung); **D**: Joint Housing; **E**: Adapter Plate; **F**: Fixing Screws; **G**: Extension Plate

Fig. 5 Schematic of the revolute joint assembly of FRS

3 Sources of Vibration in Flexible Robotic System and Its Characterization

It is to be noted that inherent vibration of the flexible robot is directly proportional to the number of degrees-of-freedom of the FRS. Accordingly, combating such vibration, in coupled form in most of the time, becomes tricky and becomes model-dependent with input from multisensory data fusion metrics. The sources of this built-in vibration in FRS can be categorized in two groups, viz., (a) *vibration: based on location of the members and* (b) *vibration: based on type of members*. Now, locationwise, sources of vibration in FRS are the following: (a) at the end-effector; (b) at the distal link; (c) at the rotary type joints, and (d) at the flexible shafts. The sources of vibration as per the type of FRS-members are the following: a] truss-based; (b) beam-based; (c) cantilever-based, and d] flexure-based. Vibration signature from the respective FRS-member, in general, will be ascertained through an ensemble of base-matrix (for housing sensing elements) and the frame of the member. For example, for truss-type members, it is the composite deflection that matters and the vibration needs to be evaluated from the interlinked structure of the particular member, as and when those are strained within elastic limit. In case of beam-based FRS-member, the FRS-member will have *microbeam* and the force-sensing mechanism will be based on beam deflection principle. Now a particular FRS-member may have multiple beams embedded in it, each having its own characterization. The placement of those beams inside the FRS-member is also another technological challenge. Besides, layout of those "beams" should also be prefixed. A standard way of placement of beam-members in FRS is matrix layout; either rectangular or circular. Nonetheless shapes other than these two can also be thought of for layout design, e.g. elliptical or triangular. In case of cantilever-based FRS-member, FRS will have one or more cantilever member, having relatively larger deflection potential at the "free" end. Cantilever-type FRS-members do possess easy potential for affixing sensing element(s) as well as better relief at the non-fixed end. So far as flexure-based design of FRS-member is concerned, the member will have multiple flexible thin sub-members, which can be parked over the same supporting frame. Flexure-members will have base sensing member in an integrated fashion. Flexure-members must necessarily be designed as well as fabricated as thin and lightweight as possible. Thus, selection of material and manufacturing method are very important for flexure-based design of FRS-members. The customized design of flexure-based members should have thin section, as best as possible.

Let us take a close look at the schematics of the vibration classification in FRS, based on the member types. Figure 6a, b present the possible variations of truss-based and beam-based link design. Locations of the strain gauges are depicted as "=" legend in Fig. 6 and afterward. Likewise, five possible variants of the cantilever-based link design are illustrated schematically in Fig. 7 comprising straight, step-straight, curvilinear, curve-straight, and arch type. By virtue of the cantilever effect, strain gauges at the respective pickup locations are more sensitive and thus effective for the FRS. In flexure-based link design, we have the combination of beam bending

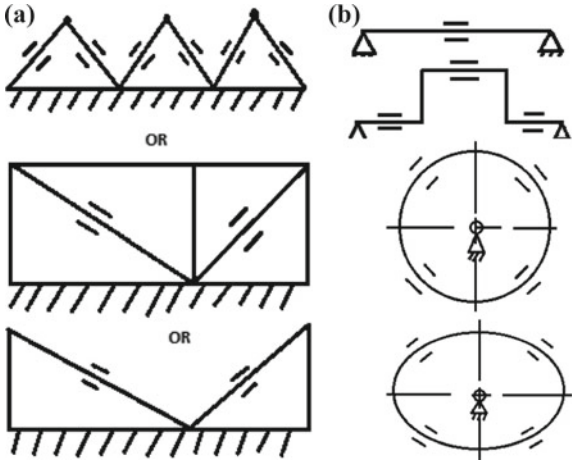

Fig. 6 Schematics of **a** Truss-based and **b** Beam-based link design of FRS (straight, circular and elliptical)

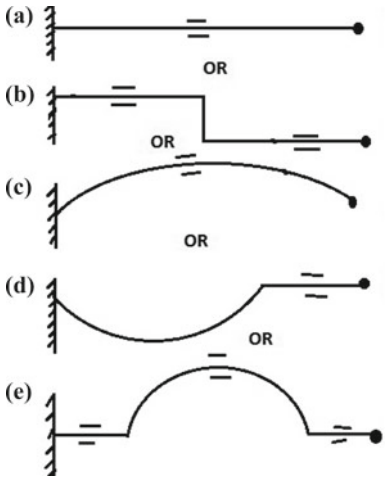

Fig. 7 Schematics of cantilever-based link design of FRS

as well as effect of cantilever together. Figure 8 schematically shows three feasible variations of this design.

With reference to Fig. 8, while scheme (a) is just an extension of the normal beam-based design, wherein the extended portion (BC) is responsible for creating the flexure Likewise, for scheme (b), we have blind-type flexure member (CD), bounded by horizontal as well as vertical beam/column members, like AB, BC, DE, and EF. Of course, it is to be noted that there will be characteristic differences between "open-ended" flexure member (like BC of scheme-a) and "blind-type" flexure member (like CD of scheme-b). Deflection of strain gauges for flexure member is interesting to be noted too. The design scheme (c) is a combination of circular beam member (BCD), open-ended flexure member (DE), and a vertical column member (AB).

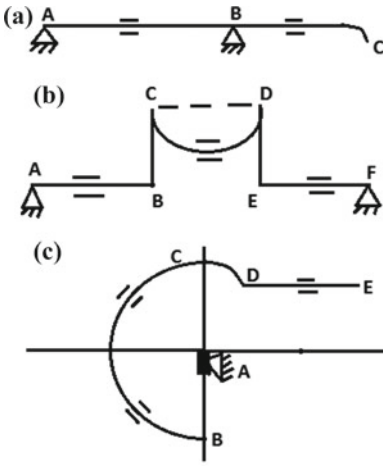

Fig. 8 Schematics of flexure-based link design of FRS

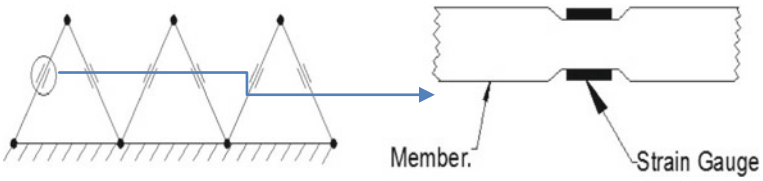

Fig. 9 Schematics of strain gauge-based vibration signature

Strain gauges and flexi-force sensors, mounted on each link of the flexible manipulator (as per design: 5 strain gauges and 2 flexi-force sensors per link) will act as prime source of detection of the vibration in real time, backed up by indigenous electronic circuitry hardware, as depicted in Fig. 9.

4 Modeling of the Damping and Dynamics of Flexible Robotic System

The multidimensionality of the in situ vibration of the FRS, as detailed out in the last section, needs subtle mathematical modeling. The spring-damper-dashpot design scheme is the most optimal tool for the vibration analysis of FRS as it has inherent uncertainties and real-time vibration control issues. As a matter of fact, this in situ vibration-based method has become prudent in design synthesis for FRS due to its in-built nature of the range of dimension of the parameters. Before detailing out the modeling scheme, we need to take a closer look at the characteristics of a FRS-member when subjected to in situ vibration (both inherent as well as external). This

phenomenon has been simulated through the actuation of various spring-elements in unison, which are attached to the FRS-member.

The FRS-body will have member(s) mounted on mechanical springs, in order to realize spring-dashpot-based modeling of the FRS-member. Thus, those as-modeled spring-mounted members will act as in situ vibration source, which will be helpful in assessing the overall deflection of the system.

The overall FRS architecture will have decent deflection scheme: the first is the inherent deflection/vibration of the mounting spring and the second one is the deflection of the links and joints. This conjugate deflection paradigm is the crux of the controller design of the FRS. It is to be noted that design of the spring-elements is a vital aspect of the design ensemble. There can be various design models of the spring-elements/members, which will be mounted/fixed directly over the link of the FRS in the model. Another interesting feature of this spring-mounted modeling structure is to have couple of "branches" (just like "tree branches") of the different spring-elements and/or spring-dashpot system. The later design model, viz., spring vibration damper (dashpot) system will be self-compensated and the resultant vibration, generated thereof, will be the optimal amount required for stimulating the FRS-ensemble.

The disposition of a specific FRS-member under in situ vibration can have several incarnations so far as damping model is concerned. Some of the feasible design ideations of this damping model are illustrated in Fig. 10. As can be observed from Fig. 10, two types are emerging, viz., (a) Type-I: horizontal member: spring mounted (Design Schemes:'A', 'D', 'E', 'F', 'G', 'H', 'I') and (b) Type-II: vertical member: spring mounted (Design schemes: 'B', 'C', 'J').

It is to be noted here that design option for vertical/column members are limited, as the layout of the springs will not undergo major variations. On the other hand, horizontal members will have number of variations possible, owing to the layout of the spring member(s). It may also be observed that the fundamental aspect of

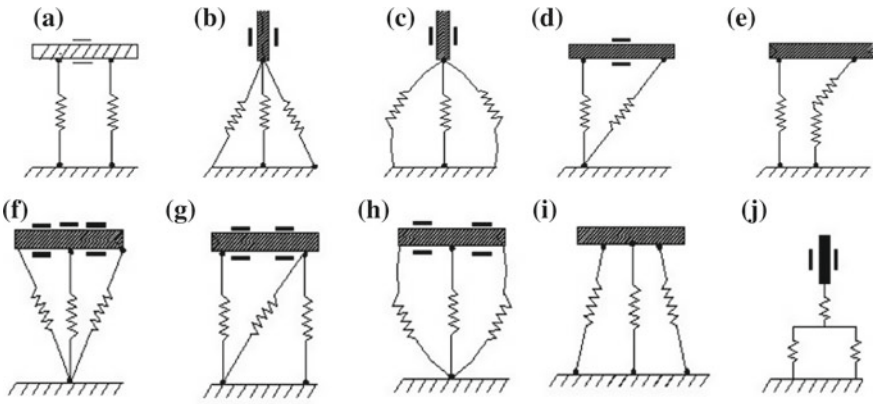

Fig. 10 Schematics of feasible modeling layouts of in situ vibration of FRS-member

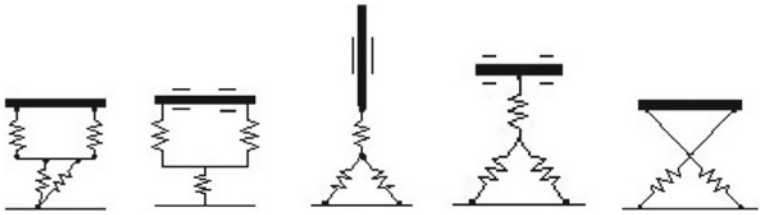

Fig. 11 Schematics of functionally bonded spring-elements under in situ vibration of FRS-member

the disposition of the spring metric (for horizontal members) is essentially multi-spring type, which is the crux of the spanning layouts. Multiple springs do give rise to options for enhanced compliance and with various permutations of spring-layout, modeling of the flexibility of the overall FRS-structure gets boosted up. Thus, both Type-I and Type-II model variants of vibration design play a big role will in characterizing the overall design ensemble of the FRS. One interesting feature of the spring-layouts shown in Fig. 10 is the individuality of the spring-elements, irrespective of the members (horizontal or vertical) thereof.

We will now deal with another layout, wherein disposition of the spring-elements can be functionally bonded and/or crisscrossed with fellow spring-element(s). Criss-crossing layout is a unique call of design, wherein two spring-members are "crossing" each other to form an ensemble. In other design layouts (refer Fig. 10) we have incorporated spring-members only in one direction, i.e., the spring rheology (tension and/or compression) was based on unidirectional arrangement. In fact, this sort of layout is entrusted to provide more subtle input to characterization of real-time damping. Figure 11 illustrates the schematic of the spring-layouts, using horizontal as well as vertical member. Let us now investigate other two types of design layouts under in situ vibration-based layout, viz., "circular-member: spring-mounted" and "elliptical member: spring-mounted". Elliptical members will have similar design layouts as of circular type. Possible design variants with circular and elliptical members are schematically shown in Fig. 12a, b (a1 and a2). Most of the features of circular-member and spring-element types (i.e. angle 2θ) remain same for elliptical members too.

The spring-damper-dashpot design theme is the most crucial aspect of flexible robotic systems due to its inherent uncertainty and real-time vibration control issues. The design model of this in situ vibration system in FRS has been schematically shown in Fig. 13.

As evident from Fig. 13, "A" and "D" have mutual sharing of kinetics, while the effect of that will be arrested by "B" and "C". Since this design is related to forcing function of spring system or spring-mass-damper system, we have enough room to imbibe the concept of interval mathematics to solve the force displacement tuple. It is true that the principles of interval mathematics can be adapted to other categories of designs as well, but we will explore the postulation with in situ vibration-based method of design first. In this context, we have for each design variable, "X" in "$\mathfrak{R}$" ('$\mathfrak{R}$': 3D space in real time), a close association of parametric range (end-values)

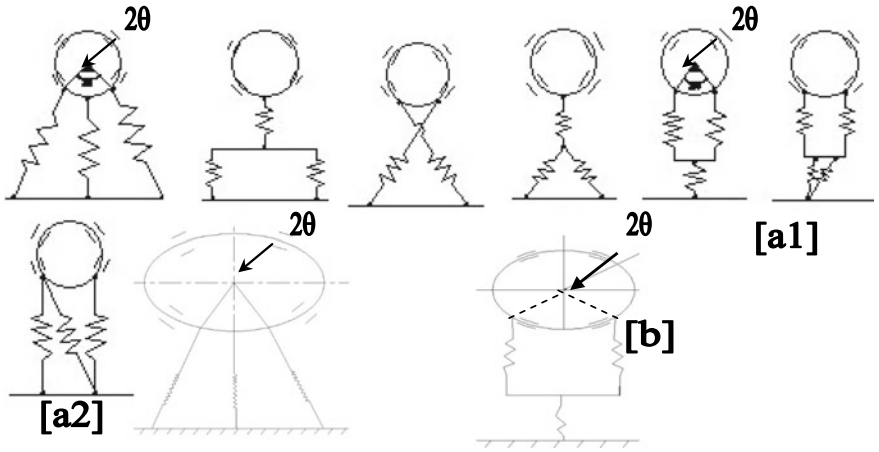

Fig. 12 Disposition schematics of (**a**) Circular and (**b**) Elliptical spring-elements under in situ vibration of FRS-member

Fig. 13 Real-life design model of in situ vibration in FRS

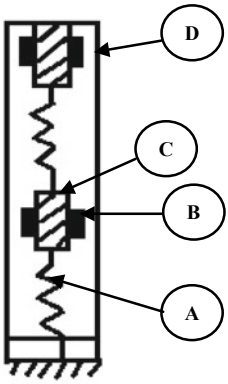

Legends:
A: 'Spring' member;
B: 'Thin-Beam' member;
C: 'Strain' member;
D: 'Membrane' member

such that $\{X\}: \rightarrow \left[\underline{X}, \bar{X}\right]$ or $\rightarrow [X_{min}, X_{max}]$ in "$\mathfrak{R}$". These two range-values of "'X" will be experimentally determined and/or simulated a priori. Hence, as explained in Fig. 13, we will have a combination of four design variables, pertaining to "A", "B", "C", and "D", which will have following paradigms:

"**A**": $\rightarrow$ {Spring-Constant} $\rightarrow \{K\}: \rightarrow \left[\underline{K}, \bar{K}\right] \rightarrow [K_{min}, K^{max}] \in \mathfrak{R}$

"B" $\rightarrow$ {Thin Beam Length and Thin Beam Width} $\rightarrow \begin{matrix}\{l\} \\ \{w\}\end{matrix} : \rightarrow \begin{bmatrix} \underline{l} & \bar{l} \\ \underline{w} & \bar{w} \end{bmatrix} \rightarrow$

$$\begin{bmatrix} l_{min} & l_{max} \\ w_{min} & w_{max} \end{bmatrix} \mathfrak{R}$$

"**C**" → {Strain gauge resistance and Gauge Length} → $\begin{matrix}\{R_{SG}\}\\ \{L_G\}\end{matrix}: \rightarrow \begin{bmatrix} \underline{R} & \bar{R} \\ \underline{L} & \bar{R} \end{bmatrix} \rightarrow$

$\begin{bmatrix} R_{SG\,min} & R_{SG\,max} \\ L_{G\,min} & L_{G\,max} \end{bmatrix} \mathfrak{R}$

"D" → {Joint Strength: Membrane} → {J$_M$}: → $\left[\underline{J_M}, \bar{J}_M\right] \rightarrow \left[J_{M\min}, J_{M\max}\right] \in \mathfrak{R}$.

The formulation and computation of these interval matrices are crucial for the calibration of the sensing elements of the FRS.

Now, while dealing with a group of design variables like in this case of FRS, "A", "B", "C", and "D" (i.e., four variables) or in expanded fashion six variables, we can define "Constraint Satisfaction Problem" (CSP). By definition, CSP is formulated by a set of variables, $\{V\} = \{x_1 \quad x_2 \ldots x_n\}$ along with a set of "Constraints" or equations $\{E\} = \{c_1 \quad c_2 \ldots c_n\}$ over interval domains: $\{[x_1] \quad [x_2] \ldots [x_n]\}$. The formulation of CSP is essentially design-specific, i.e., for a particular design of the force sensor we will have one CSP formulated. Hence, each CSP can tackle a group of new variables, pertaining to the tuple of {V} and {E}. Damping model can be established mathematically using this lemma.

5 Dynamic Control and Stability of Flexible Robotic Systems Data Analysis

The dynamic control of FRS is essentially data-driven and postulation-based, as generated from the damping model. We have designed multisensory data space for the FRS by adopting zone-based layout of the sensor-cells. The basic paradigm of the sensor placement and geometrical layout has been described in detail in an earlier work of the author on stochastic model-based hypothesis testing of sensory devices. In real-time applications (Refer: https://ieeexplore.ieee.org/document/5262650d) [23]. In-line with the modeling facets of the author, we have proposed stochastic model-based analysis of real-time vibration data of the FRS, by introducing the lemma of alternative hypothesis and null hypothesis. We define "System Dampening" as that very activity wherein the controller of FRS starts actuation and thereby initiates the full robotic cycle by maneuvering its joints. We prefer to adhere to the bimodal hypothesis paradigm and represent the inherent fuzziness in decision-making process having relatively higher value of signal-to-noise ratio [19, 20, 22].

The dynamic threshold band for ascertaining the fuzziness of committing Type-I error has been selected optimally using "Hypothesis Error Based Threshold Evaluation Method" (HEBTEM) [19]**,** wherein user-specified value of probability of Type-I error is fed as input. HEBTEM-based data analysis has been invoked in understanding the attainment of stability of the FRS in real-time. Vibration signature of FRS-members does affect a lot in determining the stability as very minute variation therein (in the order of one-thousandth) can be instrumental for dampening the FRS. The

basic paradigms of this stochastic model-based data analysis, as finetuned for the real-time control of the FRS, can be texted as follows:

(A) *Layout of the sensor-cells under multiple "zones" in the hardware of the FRS*: For example, the zones can be formulated on the basis of the placement of the sensors, viz., strain gauges, flex-force sensors, load cell and infra-red sensors. T FRS is a he optimal number of "zones" can be decided based on the physical disposition of the hardware, i.e., prototype FRS in the present case. As FRS is a jointed ensemble, the good way to decide on the "zones" is by joints. Hence we will consider a total of four zones in the model, three for the links and the rest one for the gripper of the FRS. As per the model, there can be exchange of data and/or data communication between two "neighboring" sensor-cells under a particular zone.

(B) *Postulation of the Alternative and Null Hypothesis*: Unlike the traditional way of defining statistical hypotheses, here, we propose to define the Alternative Hypothesis first. Since our primemost concern is to attenuate vibration and natural trembling of the FRS in real time, we have tested our Hypothesis when the FRS-controller achieves dampening successfully. The viability of this Alternative Hypothesis will be checked against its Null Hypothesis via Type-I error.

(C) *Inception of the Sensor Data Fusion Model*: We have established the Data Fusion model using the binary sensor-score (0 or 1) of each sensor-cell amidst all zones and the relative dependency matrix of each sensor-cell. This process is mathematical and the lemma is computational at a particular time-instant of actuation of the FRS.

(D) *Evaluation of the Dynamic Threshold Band of the Decision-zone about the Acceptance of the Hypothesis*: The probability curve of the Alternative Hypothesis does play a crucial role in evaluating this threshold band. The evaluation semantic is mathematical and the numerical value of the threshold band depends on the level of confidence in determining Type-I error.

The ensemble process of vibration control of FRS is dependent equally on all of the modules, mentioned above. Nonetheless, the actual phenomena of vibration attenuation may get vary on the choice of the Fusion Model. It has been found from earlier test-results that zonal influence-driven data fusion model works pretty effective in sensory data assimilation of real-life robotic systems. The practicality involved in such modulation is imperative that drives the fusion model in making decision on the goal of vibration control of the FRS.

6 Simulation of Flexible Robotic Systems: Analysis of Vibration and Hardware Set-up

The serial-chain flexible robotic systems, as shown in Figs. 1 and 4, were modeled in 3D and finite element analysis (FEA) was performed in order to obtain the natural frequencies of vibration of the gripper under different modes. Due to the slenderness

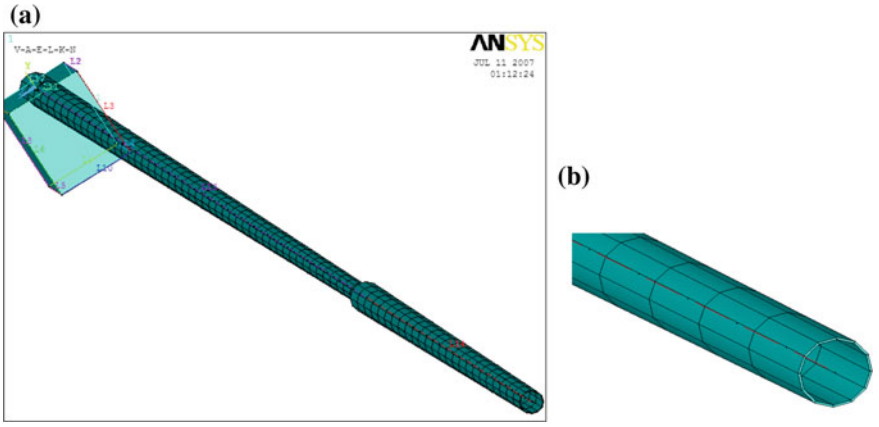

Fig. 14 Finite element model of the two-link serial-chain FRS: **a** Detailed view; **b** Magnified view

of the FRS designed, meshing for the FEA gets critical. Modal analysis of the FRS was carried out with the meshed layouts in order to obtain natural frequencies of vibration. The other important aspect that gets revealed is related to the characteristics of vibration for a "closed-chain" structure of the FRS. We will examine the differences in FEA-model as well as vibration signature for both serial-chain and closed-chain FRS. We will also highlight the effect of this inherent vibration on the gripper-end. For the FEA, we have selected two materials, viz., Kevlar and Carbon Fibre Reinforced Plastic (CFRP). FEA has been made and simulated thereof for both these materials in order to obtain the relative advantage of those in real-life firmware of the FRS. Although closed-chain FRS is a bit advantageous for the control of inherent vibration due to its structural robustness, serial-chain FRS is also competitive. The piece-wise approximation of the physical domain of the FRS provides good precision even with simple approximating functions in the FEA that was invoked. Figure 14 illustrates the FE-model of the two-link serial-chain FRS.

Figure 15 illustrates the FEA-model of the three-link FRS. The finite element analysis was carried out using the following data, viz. (a) modulus of elasticity (for CFRP: 77,000,000 Psi or 531 kN/mm^2 or 531 GPa and for Kevlar: 18,000,000 Psi or 125 kN/mm^2 or 125 GPa); (b) Shear modulus (for CFRP: 750 N/mm^2 and for Kevlar: 1540 N/mm^2); (c) Density (for CFRP: 1.75 gm/cc and for Kevlar: 1.44 gm/cc) and (d) Tensile strength (for CFRP: 820,000 Psi or 5,656 N/mm^2 and for Kevlar: 525,000 psi or 3621 MPa or 3621 N/mm^2). Linear 2-node "BEAM 188" (3D linear finite strain beam) element was used for the modeling of the links of the FRS which has got six degrees-of-freedom at each node. On the other hand, "COMBIN7" (3D pin or revolute joint) element was used to connect the links through revolute joints in the finite element model. Capabilities of "COMBIN7" include optimal modeling for joint flexibility (or stiffness), friction, damping and certain control features. Besides, this element possesses large deflection capability, by which a fixed local coordinate system can move with the joint. In order to benchmark the vibration

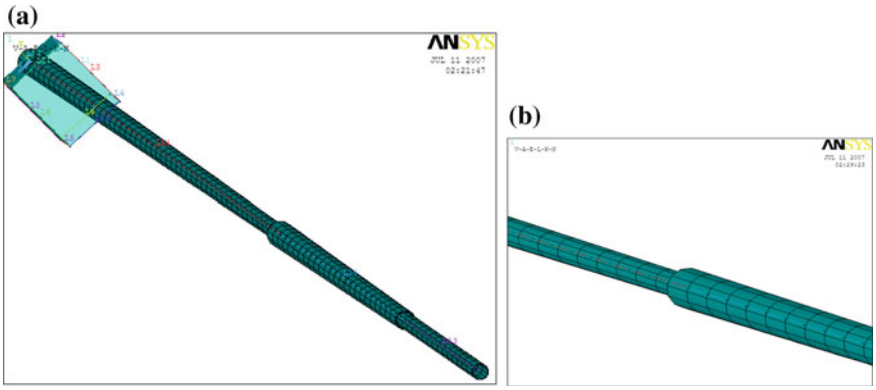

Fig. 15 Finite element model of the three-link FRS: **a** Overall meshing and **b** Zoomed view of the mesh

signature of multi-link FRS, FEA was carried out for closed-chain design of FRS too. The schematic disposition of a typical closed-chain FRS, geometric design details of its links and its ensemble mesh are presented in Fig. 16a, b, respectively. It is to be noted that mesh-model for the joint in closed-chain FRS is crucial, unlike the case of serial-chain FRS, which is similar to a "T-joint" (refer Fig. 17b).

Both serial-chain and closed-chain configuration of FRS have been simulated for FEA under vibration mode in order to evaluate the natural frequencies of vibration under different modes. Primary vibrational analysis has been made in modal solution module, so as to identify the natural frequencies and the response behavior of the

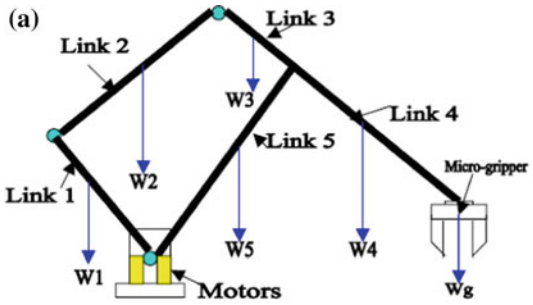

(b)

Part	Length	Volume	Mass
Link 1	625 mm.	426.84 cc	747 gm.
Link 2	700.4 mm.	478.33 cc	837 gm.
Link 3	312.5 mm.	213.42 cc	373.5 gm.
Link 4	625 mm.	426.84 cc	747 gm.
Link 5	625 mm.	426.84 cc	747 gm.

Fig. 16 Schematic disposition of closed-chain FRS: **a** Overall layout and **b** Design details of the links

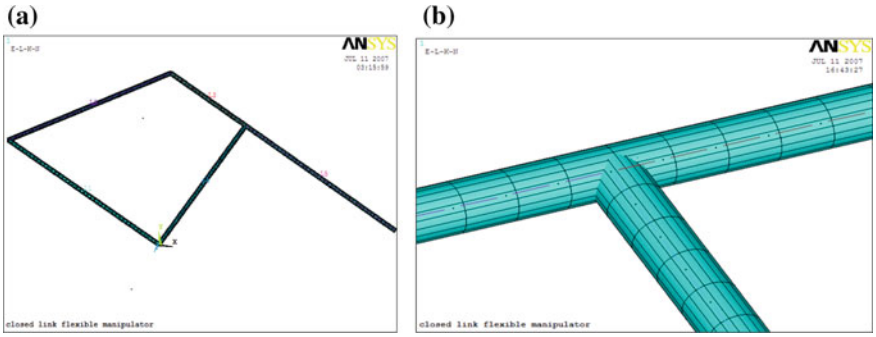

Fig. 17 FEA-Screenshot of the closed-chain FRS: **a** Ensemble mesh and **b** Model for the link-joint

FRS-structure to it. Modal analysis does not take any load data into account; it only requires a constrained body having mass defined. The study has been categorized for both CFRP and Kevlar, which educates us about the relative preference for the selection of the material for manufacturing. Natural frequencies of vibration have been evaluated through FEA for both two-link and three-link structure of the serial-chain FRS as well as for the closed-chain FRS. Table 1 presents some representative values of the natural frequency of vibration for these three layouts of the FRS. The ensemble contains 25 data-set from the initiation of the simulation and 15 data-sets from the trailing side. This has been made judiciously so as to bring out the relative alteration in the numerical values of the natural frequencies of vibration. The data-set revels that although serial 3-link FRS has got higher natural frequencies of vibration till sixth time-step over its two-link counterpart, it gets dampened over the higher time-steps. Closed-chain configuration of FRS shows even better result with reduced values of the natural frequencies of vibration, barring few initial time-steps. Likewise, Kevlar shows slightly better results over CFRP for all models of FRS so far as the inherent vibration of the system is concerned.

The FEA-based simulation of various varieties of FRS has made a strong foundation for the hardware manifestation of the systems. So far as application of the FRS is concerned, the "end-effector" of the gripper plays a salient role. We have successfully developed two variants of serial-chain FRS having revolute joint-actuated three non-identical links and one miniaturized gripper at the end of the distal link. Figures 18 and 19 illustrate the developed hardware for the FRS-variants. The FRS, shown in Fig. 18 is actuated by servomotors placed at the joints unlike the other hardware shown in Fig. 19, wherein the actuation has been achieved via flexible shafts. The designs of the grippers are also novel and quite diverse from one another. Since the prototype FRS of Fig. 18 is of a large horizontal span of 1.5 m, the photographic view is shown in four subassemblies, i.e., Fig. 18a–d. Overall disposition of the experimental hardware of the flexible shaft-actuated FRS is shown in Fig. 19a.

Table 1 Natural frequency of vibration of serial-chain and closed-chain flexible robotic system

Time-step	Natural frequency (material: CFRP) [Hz.]			Natural frequency (material: kevlar) [Hz.]		
	Serial 2-link	Serial 3-link	Closed-chain	Serial 2-link	Serial 3-link	Closed-chain
1	0.24603×10^{-3}	0.80204×10^{-4}	0.0568×10^{-3}	0.04607×10^{-3}	0.14606×10^{-3}	0.42799×10^{-2}
2	0.13009×10^{-1}	15.595	45.281	0.78792×10^{-2}	0.15640×10^{-1}	24.221
3	21.529	89.759	57.458	11.515	8.3414	30.734
4	122.16	158.57	76.578	65.342	48.012	40.959
5	160.42	249.73	114.24	85.801	84.811	61.118
6	354.51	442.79	134.31	189.63	133.58	71.836
7	522.29	515.26	286.68	279.36	236.85	153.34
8	708.07	464.40	314.17	378.73	275.59	168.04
9	994.15	540.40	395.56	531.74	401.24	211.57
10	1118.4	750.12	523.89	598.22	467.63	280.21
11	1246.6	874.29	534.04	666.74	580.77	285.69
12	1664.5	1085.8	618.84	890.36	635.76	331.02
13	1753.5	1188.6	727.55	937.94	829.06	389.16
14	2003.8	1550.0	734.27	1071.8	858.04	392.74
15	2365.6	1604.2	952.97	1265.3	980.74	509.77
16	2894.7	1833.6	1161.8	1548.3	1085.3	621.38
17	2949.1	2029.1	1457.8	1577.4	1097.0	779.78
18	3082.5	2051.0	1460.3	1648.7	1360.9	781.06
19	3296.7	2544.4	1577.2	1763.3	1401.9	843.59
20	3938.4	2620.8	1837.8	2106.6	1503.3	982.96
21	4436.3	2810.5	1914.3	2372.8	1721.5	1023.9
22	4986.2	3218.6	1992.4	2667.0	1754.8	1065.7
23	5498.6	3280.7	2147.3	2941.1	2116.5	1148.6
24	5766.6	3956.9	2188.5	3084.4	2356.8	1170.5
25	6012.0	4406.3	2587.5	3215.6	2577.4	1384.0
46	18362.0	12306.0	7273.5	9821.6	6931.7	3890.4
47	19889.0	12959.0	7474.8	10638.0	7257.9	3999.3
48	20014.0	13569.0	7744.7	10705.0	7574.3	4142.4
49	20309.0	14161.0	8143.0	10863.0	7996.6	4357.0
50	20426.0	14951.0	8402.7	10926.0	8050.5	4495.1
51	21035.0	15051.0	8688.1	11251.0	8643.1	4647.0
52	22257.0	16159.0	8740.0	11905.0	8770.5	4674.7

(continued)

Table 1 (continued)

Time-step	Natural frequency (material: CFRP) [Hz.]			Natural frequency (material: kevlar) [Hz.]		
	Serial 2-link	Serial 3-link	Closed-chain	Serial 2-link	Serial 3-link	Closed-chain
53	22566.0	16397.0	8816.1	12070.0	9092.3	4716.5
54	23314.0	16999.0	9374.4	12470.0	9207.7	5014.1
55	24565.0	17215.0	9558.5	13140.0	9676.1	5112.7
56	26205.0	18090.0	9949.4	14016.0	10195.0	5322.1
57	26343.0	19061.0	10140.0	14090.0	10476.0	5423.8
58	26813.0	19586.0	10299.0	14341.0	10720.0	5508.6
59	26843.0	20041.0	10562.0	14358.0	10740.0	5649.4
60	27700.0	20080.0	11125.0	14816.0	11271.0	5951.1

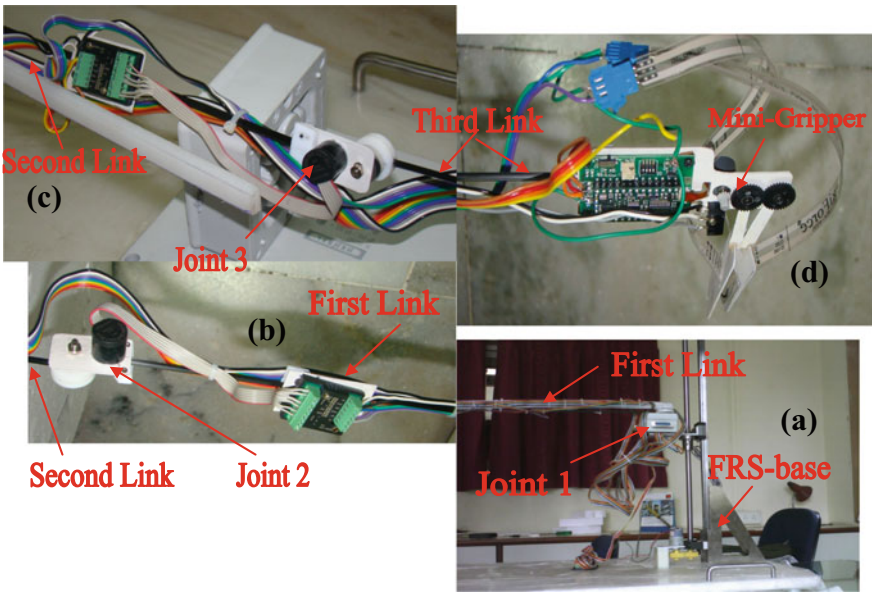

Index: [a]: FRS-base, joint 1 & a part of FRS-first link; [b]: A part of FRS-first link, joint 2 & partial view of the FRS-second link; [c]: Partial views of FRS-second & FRS-third links & joint 3; [d]: A part of FRS-third link & mini-gripper

Fig. 18 Prototype of the three-link serial-chain "direct drive" flexible robotic system with miniaturized gripper

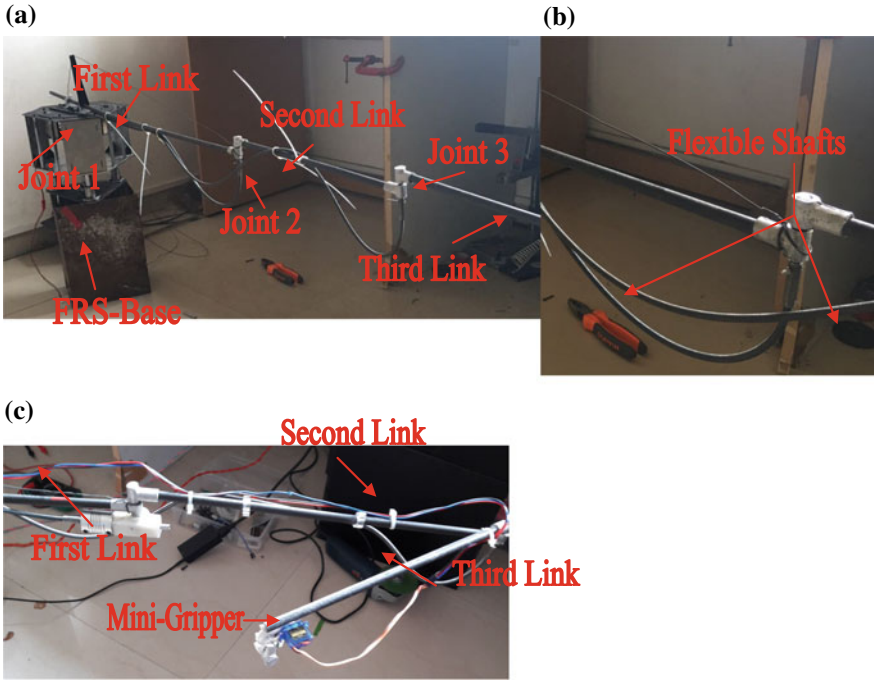

Fig. 19 Experimental hardware of the three-link serial-chain "flexible shaft"-driven FRS with mini-gripper

Flexible shafts, responsible for actuating joints 2 and 3 are zoomed in Fig. 19b and interfacing of the mini-gripper with the FRS is snapped in Fig. 19c.

7 Conclusions

We propose new models for in situ vibration signature of a multi-link flexible robotic system using spring-dashpot-damper and strain gauges. The vibration characteristic of multi-link FRS is quite different from that of single link flexible robots due to the coupling effects of joints and flexible shafts. Although the natural frequencies of vibration of FRS are dependent on the layout of the FRS (serial-chain vs. closed-chain) and its material of construction, the significant contribution does emanate from the drive system of the FRS-joints and run-time program. Scientifically ascertained locations of augmentation of strain gauges on the FRS-links play a crucial role too in the overall target of achieving smoother control of the system dynamics. The present research builds up an optimal foundation for analyzing inherent vibration of flexible robots using strain gauge-based measurement as well as stochastic model-based fusion of sensory data.

Acknowledgements Author acknowledges the help rendered by Shri Stianshu Das, B.Tech. student of Indian Institute of Technology, Kharagpur in performing Finite Element Analysis of the FRS structures as part of his internship project. The technical assistance provided by the engineers of M/s Devendra Fabricators, Nashik, Maharashtra and M/s SVR Infotech, Pune, Maharashtra is duly acknowledged pertaining to the fabrication of the serial-chain flexible robotic systems.

References

1. Benosman M, Vey G (2004) Control of flexible manipulators: a survey. Robotica 22(2004):533–545
2. Fraser AR, Daniel RW (1991) Perturbation techniques for flexible manipulators. Norwell, MA, Kluwer
3. Luo ZH (1993) Direct strain feedback control of a flexible robot arm: new theoretical & experimental results. IEEE Trans Autom Control 38(11):1610–1622
4. Chen Wen (2001) Dynamic modeling of multi-link flexible robotic manipulators. Comput Struct 79(2):183–195
5. Feliu V, Somolinos JA, Garcia A (2003) Inverse dynamics based control system for a three degrees-of-freedom flexible arms. IEEE Trans Robot Autom 19(6):1007–1014
6. Feliu V, Ramos F (2005) Strain gauge based control of single-link flexible very light weight robots robust to payload changes. Mechatronics 15:547–571
7. Subudhi B, Morris AS (2002) Dynamic modeling, simulation and control of a manipulator with flexible links and joints. Robot Auton Syst 41(4):257–270
8. Moudgal VG, Kwong WA, Passino KM, Yurkovich S (1995) Fuzzy learning control for a flexible-link robot. IEEE Trans Fuzzy Syst 3(2):199–210
9. Singer NC, Seering WC (1990) Preshaping command inputs to reduce system vibration. J Dyn Syst Meas Control Trans ASME 112:76–82
10. Chen YP, Hsu HT (2001) Regulation and vibration control of an fem-based single-link flexible arm using sliding-mode theory. J Vib Control 7(5):741–752
11. Tjahyadi H, Sammut K (2006) Multi-mode vibration control of a flexible cantilever beam using adaptive resonant control. Smart Mater Struct 15:270–278
12. Trapero-Arenas JR, Mboup M, Pereira-Gonalez E, Feliu V (2008) Online frequency and damping estimation in a single-link flexible manipulator based on algebraic identification. In: Proceedings of the 16th mediterranean conference on control and automation (IEEE). Franco, pp 338–343
13. Pereirea Emiliano, Aphale Summet Sunil, Feliu Vicente, Moheimani SOR (2011) Integral resonant control for vibration damping and precise tip-positioning of a single-link flexible manipulator. IEEE/ASME Trans Mechatron 16(2):232–240
14. Zhang J, Tian Y, Zhang M (2014) Dynamic model and simulation of flexible manipulator based on spring and rigid bodies. In: Proceedings of the 2014 IEEE international conference on robotics and biomimetics ('ROBIO-2014'), pp 2460–2464
15. Chair Z, Varshney PK (1986) Optimal data fusion in multiple sensor detection systems. IEEE Trans Aerosp Electron Syst AES-22(1):98–101
16. Thomopoulos SCA, Viswanathan R, Bougoulias DC (1987) Optimal decision fusion in multiple sensor systems. IEEE Trans Aerosp Electron Syst AES-23(5):644–653
17. Kam M, Chang W, Zhu Q (1991) Hardware complexity of binary distributed detection systems with isolated local bayesian detection. IEEE Trans Syst Man Cybern SMC-21(3):565–571
18. El-Ayadi MH (2002) Nonstochastic Adaptive Decision Fusion in Distributed-Detection Systems. IEEE Trans Aerosp Electron Syst 38(4):1158–1171
19. Roy Debanik (2007) Estimation of grip force and slip behavior during robotic grasp using data fusion and hypothesis testing: case study with a matrix sensor. J Intell Robot Syst 50(1):41–71

20. Roy D (2008) Stochastic model-based grasp synthesis: new logistics for data fusion with dissimilar sensor-cells. In: Proceedings of the IEEE international conference on automation and logistics (IEEE-ICAL 2008). Qingdao, China, pp 256–261
21. Roy D (2009) A new fusion rule-base for slender tactile cells in a homogeneous robotic slip sensory grid. In: Proceedings of the IEEE international conference on robotics and biomimetics (IEEE-ROBIO 2008). Bangkok, Thailand
22. Roy D (2009) A new fusion rule with dynamic decision threshold for heterogeneous field gripper sensory system: Part I. In: IEEE/RSJ international conference on intelligent robots and systems (IROS 2009). USA
23. Roy D (2009) A new fusion rule with dynamic decision threshold for heterogeneous field gripper sensory system: Part II. In: Proceedings of the IEEE international conference on automation and logistics (IEEE ICAL 2009). China